Preparation and characterization of pure and KBr doped polymer blend (PVC/PEO) electrolyte thin films

N. Reddeppa [a,b,*], A.K. Sharma [b], V.V.R. Narasimha Rao [b], Wen Chen [a]

[a] State Key Laboratory of Advanced Technology for Materials Synthesis and Processing, and School of Materials Science and Engineering, Wuhan University of Technology, Wuhan 430070, People's Republic of China
[b] Sri Venkateswara University, Department of Physics, Tirupati 517502, India

ABSTRACT

A potassium ion conducting polymer blend electrolyte based on polyvinyl chloride (PVC) and polyethylene oxide (PEO) complexed with KBr was prepared using solution cast technique. The structural properties of these electrolyte films were examined by XRD studies. The XRD data revealed that the amorphous domains of polymer blend matrix increased with increase of KBr salt concentration. The complexation of the salt with the polymer blend was confirmed by FT-IR studies. Electrical conductivity of the films was measured with impedance analyzer in the frequency range of 100 Hz to 1 MHz and in the temperature range of 303–363 K. It was observed that the magnitude of conductivity increased with the increase in the salt concentration as well as the temperature. UV–VIS absorption spectra in wavelength region of 200–600 nm were used to evaluate the optical properties like direct band gap, indirect band gap and absorption edge. The optical band gaps decreased with increasing of K^+ ion concentration. This suggests that, KBr is a good dopant to improve the electrical properties of PVC + PEO polymer blend electrolytes. Studies on the electrical and optical properties of polymer blend electrolyte have attracted much attention in view of their application in electronic and optical devices like electro-chromic display devices, fuel cells, gas sensors and solid state batteries. The thermal properties of these films were investigated with differential scanning calorimetry (DSC). The variation in film morphology is examined by scanning electron microscopy examination (SEM).

1. Introduction

Ionic polymer complexes are scientifically interesting owing to their possible wide range of applications in solid state electrochemical devices such as energy conversion units (batteries/fuel cells), electrochemical display devices/smart windows, photoelectrochemical cells, etc. PVC is a commercially available inexpensive polymer and is compatible with a large number of plasticizers, such as ethylene carbonate (EC), propylene carbonate (PC), dibutyl phthalate (DBP) and dioctyl adipate (DOA). Several researchers have reported plasticized polymer electrolytes with enhanced ionic conductivity in PVC based polymer electrolytes [1–4]. Poly(ethylene oxide) (PEO) is the most popular polymer, which solvates the high concentration of ionic salts [5–9]. Ionic salt with PEO has been the subject of interest in polymer electrolytes, where the transient cross-links between the cations and ether oxygen of PEO play the major role to facilitate ion disassociation. Most of the reported solid polymer electrolytes (SPEs) are based on alkali metal salts [10–15]. Utilization of solid polymer electrolytes in electrochemical devices depends on various factors like mechanical, thermal properties and ionic conductivity. To enhance the ionic conductivity many approaches are in use [16–19]. The main advantages of the blend based polymer electrolytes are simplicity in preparation and easy control of physical properties by compositional change. PEO–salt complexes studied extensively other than the lithium-based polymer electrolytes.

Solid polymer electrolyte materials are attracting growing interest in recent years because of their potential applications in ionic devices such as rechargeable batteries, supercapacitors and gas sensors [17–19]. Polymer materials are used in solid state battery system because of better mechanical properties, ease of fabrication as thin films and their ability to form good contact with electrode material. From an electrochemical point of view, the electrolyte should satisfy a set of requirements. They include high ionic conductivity, wide electrochemical stability and chemical/electrochemical compatibility with electrode material.

Over the past few years, many polymeric electrolytes based on various salts dissolved in polyethers, particularly poly(ethylene

* Corresponding author at: State Key Laboratory of Advanced Technology for Materials Synthesis and Processing, and School of Materials Science and Engineering, Wuhan University of Technology, Wuhan 430070, People's Republic of China. Tel.: +86 27 87160129; fax: +86 27 87864580.
E-mail address: reddeppa.svu@gmail.com (N. Reddeppa).

oxide) (PEO) have been widely investigated because of their potential viability in high-performance batteries [20,21]. Such electrolytes have been based mainly on alkali metal salt systems [14,15]. Special attention has been focused on lithium [22–24]. Less effort has been made on solid polymer blend electrolytes and batteries based on potassium complex systems. Apart from scientific interest, the use of potassium has several advantages over lithium counterparts. Potassium is much more abundant and less expensive than lithium. The softness of this metal makes it easier to achieve and maintain good contact with other components in the battery. Further, potassium is more moisture–resistant than lithium. Keeping these aspects in view, this study reports a new K$^+$ ion conducting polymer blend electrolyte system based on polyethylene oxide (PEO) and polyvinyl chloride (PVC) complexed with potassium bromide (KBr).

2. Experiment procedure

Films (thickness ≈100 μm) of pure blends of PVC + PEO (Aldrich, MW 6×10^4 and 6×10^5) and various compositions of complexed films of (PVC + PEO) with a salt of KBr were prepared in the weight percent ratios (47.5:47.5:5), (45:45:10) and (42.5:42.5:15) by solution cast technique using tetrahydrofuran (THF) as a solvent. The solutions were stirred for 10–12 h to get a homogeneous mixture and then cast onto polypropylene dishes and evaporated slowly at ambient atmosphere. The final product was vacuum dried thoroughly at 0.13 Pa.

In order to investigate the nature of these polymer blend electrolyte films, X-ray diffraction studies were carried out using HLG4/B-PC X-ray diffractometer with Cu Kα radiation and graphite monochromator at room temperature. FT-IR spectra of these films were recorded using EO-SXB IR spectrometer with a resolution of 4 cm^{-1}. The measurements were taken over the wave number range 400–4000 cm^{-1}. Differential scanning calorimetry (DSC) measurements were carried out on using NETZSCH DSC 204 in the range 50–75 °C, and all the measurements were taken at a heating rate of 10 °C min^{-1} under nitrogen atmosphere. AC impedance measurements were performed by using Hioki 3532-50 LCR Hi-Tester interfaced to a computer in the frequency range 100 Hz–1 MHz and temperature range 303–363 K. The morphology of the samples was characterized by JOEL JSM 840A electron microscope with scanning attachment was used for the SEM studies of polymer blend electrolyte system. Optical absorption spectra were recorded at room temperature in the wavelength region 200–600 nm using Shimadzu UV–VIS–NIR (Model UV-3100) spectrophotometer. From these data the optical constants such as band edge, optical band gap (both direct and indirect) were determined.

3. Results and discussion

3.1. X-ray diffraction analysis

Fig. 1(a)–(e) shows the X-ray diffraction (XRD) patterns of pure PVC + PEO, KBr salt and PVC + PEO complexed with KBr salt. XRD patterns of KBr salt shows well defined peaks at around $2\theta = 23°$, 55°, 58° and 66° indicating its crystalline nature. However these peaks disperse in complexed polymer blend films. Pure PVC + PEO blend film exhibits two crystalline peaks of PEO, a maximum intensity peak at 19.2°, next maximum peak at 23.6°. Fig. 1(a) shows one broad peak at angle $2\theta = 13°$, which corresponds to PVC. The semicrystalline nature of PVC structure is disturbed by the addition of PEO and salt. No such well defined sharp peaks attributable to PVC could be observed. These observations confirm that the present polymer blend system is multiphase, possessing both crystalline and amorphous regions. However, on the addition of the salt
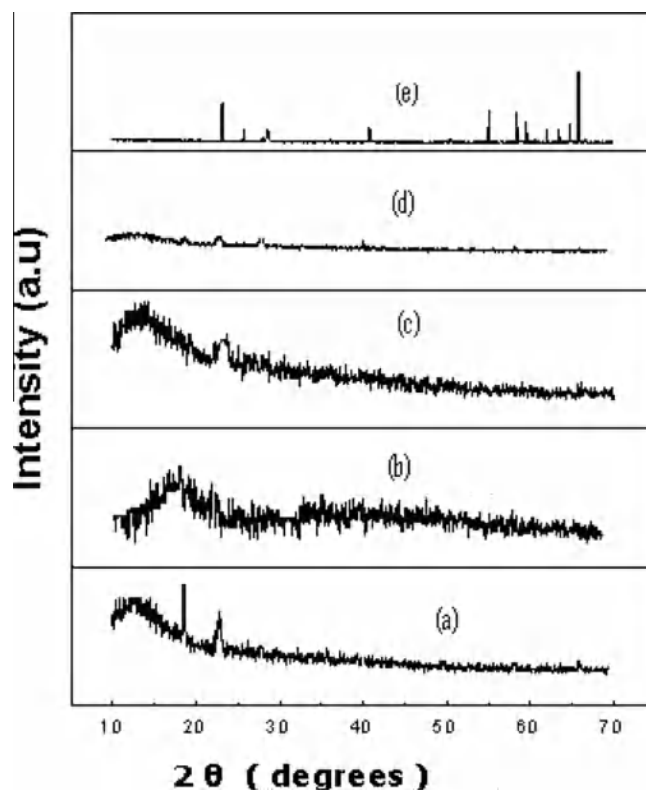

Fig. 1. XRD patterns of (a) pure PVC + PEO; (b) PVC + PEO + KBr (47.5:47.5:5); (c) PVC + PEO + KBr (45:45:10); (d) PVC + PEO + KBr (42.5:42.5:15); (e) KBr salt.

to the polymer blend, the intensity of the peaks decreases gradually and becomes relatively broader, suggesting that a decrease in the degree of crystallinity of the complex. Hodge et al. [25] established a correlation between the intensity of the peak and the degree of crystallinity. They observed that the intensity of diffraction patterns decreases as the amorphous nature increases with the addition dopant. In the present XRD patterns, no sharp peaks were found for higher concentrations of KBr salt in the polymer blend, indicating the presence of dominant amorphous phase [26]. This amorphous nature results in greater ionic diffusivity with high ionic conductivity, as amorphous polymers have flexible backbone [27]. Absence of peaks pertaining to potassium bromide salt in the complexes indicates the complete dissolution of salt in the polymer matrix.

3.2. FTIR analysis

FT-IR spectroscopy is important in the investigation of polymer structure, since it provides information about the complexation and interactions between the various constituents in the polymer blend electrolyte system. The FTIR spectra of pure PVC + PEO, KBr and polymer blend complexes are shown in Fig. 2(a)–(c). The following changes in the spectral features were observed after comparing the spectrum of complexed PVC + PEO with that of pure PVC + PEO and KBr. In (PVC + PEO) the bands of spectrum in the region of 600–700 cm^{-1} are characteristic of C–Cl stretching vibrations of PVC. The vibrational frequency at 1279 cm^{-1} assigned to C–O stretching of PEO in polymer blend. The intensity of the aliphatic C–H stretching band observed around 2900 cm^{-1} in PEO is found with 10 wt% concentration of KBr salt in the polymer blend. The width of the C–O stretching band observed around 1100 cm^{-1} in PEO also showed a decrease with an increase of KBr in the polymer blend. The decrease in the width of the 1100 cm^{-1} band,
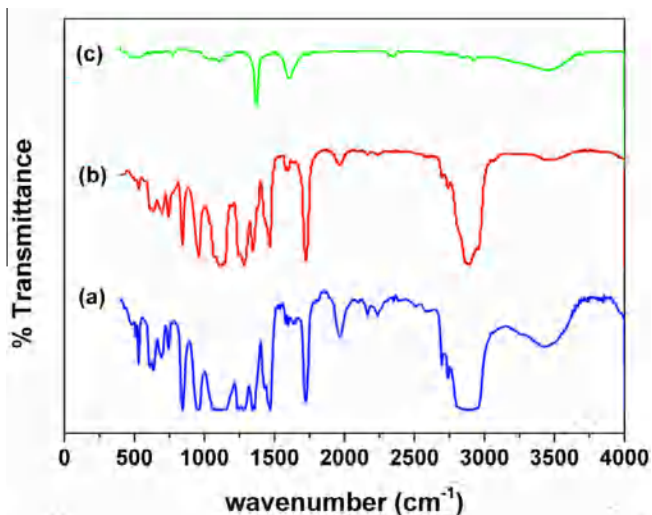
Fig. 2. FTIR spectra of (a) pure PVC + PEO; (b) PVC + PEO + KBr (45:45:10); (c) KBr salt.

which is assigned to C–O–C symmetrical and asymmetrical stretching [28], suggests the co-ordination/complexation of the salt with PEO. The band at 1085 cm^{-1} is assigned to C–H rocking vibration of PVC, which gets shifted to 1062, 1064 and 1147 cm^{-1} in polymer blend complex respectively (Fig. 2(b)). CH$_2$ deformation vibration band is observed at 1468 cm^{-1} in pure polymer blend, which gets shifted to 1469, 1467 and 1468 cm^{-1} in polymer blend complexes due to complexation of the salt. The characteristic frequencies of KBr salt at 625, 1347 and 1640 cm^{-1} are shifted to 637, 1344 and 1467 cm^{-1} in the polymer blend complexes respectively. These results suggest that homogeneous polymer electrolytes are formed over all the blend compositions.

3.3. Impedance analysis

The complex impedance plot of PVC + PEO + KBr (42.5:42.5:15) polymer blend electrolyte at different temperatures is shown in Fig. 3. This figure shows two well defined regions; a high frequency semicircle related to the parallel combination of a resistor and a capacitor and a low frequency spike representing formation of
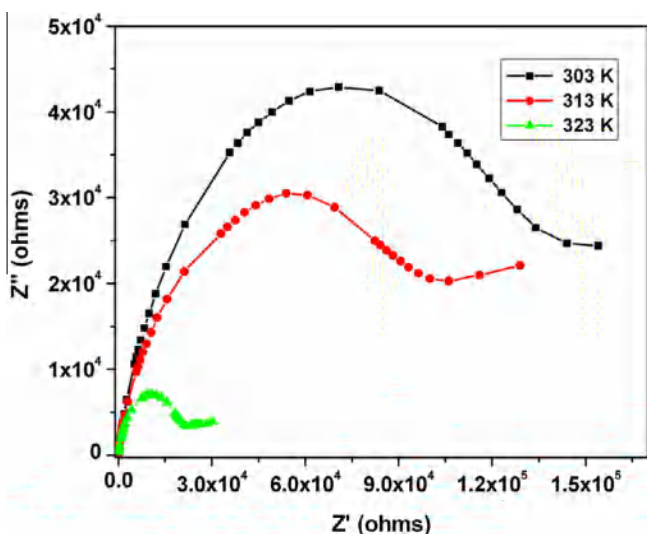
double layer capacitance at the electrode–electrolyte interface due to migration of ions at low frequency. The low frequency response appearing as an inclined spike at an angle less than 90° to the real axis indicates the inhomogeneous nature of the electrode–electrolyte interface. The bulk resistance of the polymer blend electrolytes at different temperatures was obtained by the intersection of semicircle with the real axis. It can be seen from Fig. 3 that the magnitude of bulk resistance decreases with increase in temperature.

Ionic conductivity of the solid polymer blend electrolyte was calculated from the measured bulk resistance, area and thickness of the polymer film using Eq. (1):

$$\sigma = L/R_b \times A \qquad (1)$$

where L is the thickness of the polymer blend electrolyte (cm), A is the area of the blocking electrode (cm^2) and R_b is the bulk resistance of polymer blend electrolyte. At ambient temperature, the highest ionic conductivity value was found to be 2.56×10^{-5} S cm^{-1} for PVC + PEO + KBr (42.5:42.5:15) polymer blend electrolyte. The conductivity of pure (PVC + PEO) was 3.09×10^{-6} S cm^{-1} at room temperature and its value increased about 10 times on complexing it with 15% KBr, as the rise of conductivity is significant with increased concentration of KBr.

It is observed that as the temperature increases the conductivity also increases for all the complexes and this behavior is agreement with the theory established by Croce et al. [29]. This is rationalized by recognizing the free volume model [4]. When the temperature increased, the vibrational energy of a segment is sufficient to push against the hydrostatic pressure imposed by its neighboring atoms and create a small amount of space surrounding its own volume in which vibrational motion can occur [30]. Hence the increment of temperature causes the increase in conductivity due to the increased free volume and their respective ionic and segmental mobility.

The DSC curves of pure PVC + PEO and PVC + PEO complexed with KBr at a (47.5:47.5:5) and (42.5:42.5:15) composition are shown in Fig. 4. An endothermic peak is observed at 65.5 °C, which corresponds to the melting temperature of pure PVC + PEO. The slight shift in the melting point T_m, toward lower temperatures is due to the addition of KBr salt to the polymer blend. In addition, the melting endotherm is found to broadened with increase of salt concentration. The decreasing in the melting temperature and the broadening of the melting endotherm are clear indications of de-

Fig. 3. Impedance plots (Cole–Cole) for PVC + PEO + KBr (42.5:42.5:15) polymer blend electrolyte at different temperatures.
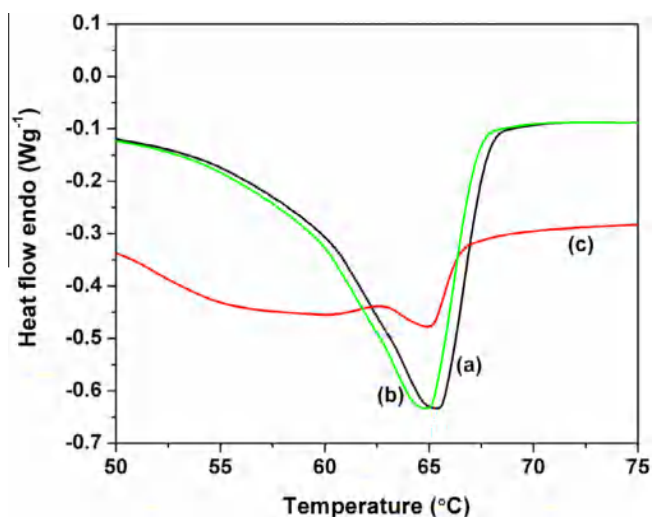

Fig. 4. DSC curves of (a) pure PVC + PEO; (b) PVC + PEO + KBr (47.5:47.5:5); (c) PVC + PEO + KBr (42.5:42.5:15).

crease in the degree of crystallinity and dominant presence of amorphous phase. The variation of conductivity as a function of temperature for different compositions of (PVC + PEO + KBr) polymer blend electrolyte system along with pure PVC + PEO is given in Fig. 5 for the temperature range 303–363 K at various temperatures while the conductivity data at different temperature is presented in Table 1.

The following features are observed:

1. In the temperature range of study, the conductivity increases with increase in temperature for polymer blend PVC + PEO and for all compositions of the (PVC + PEO + KBr) polymer blend electrolyte system.
2. The conductivity–temperature plots follow an Arrhenius behavior throughout, but with two regions (region-I and II), above and below melting point (T_m) of the polymer blend (marked in Fig. 5 as a vertical dotted line).

In region-I (i.e. below T_m), the conductivity slowly increases with temperature up to 65.5 °C. At this temperature, there is a sudden increase in conductivity. In the region-II (i.e. above T_m), the

Fig. 5. Temperature dependent conductivity of (a) pure PVC + PEO (50:50); (b) PVC + PEO + KBr (47.5:47.5:5); (c) PVC + PEO + KBr (45:45:10); (d) PVC + PEO + KBr (42.5:42.5:15).

conductivity again increases with temperature. Similar behavior has been observed in all the compositions of PVC + PEO + KBr polymer blend electrolyte system. The temperature (T_m), which corresponds to the melting point (65.5 °C) of the polymer blend, there is a change from a semi crystalline to an amorphous phase. Due to this phase change, the conductivity shows a sudden increase at T_m. The increase of conductivity with temperature is interpreted as being due to a hopping mechanism between coordinating sites, local structural relaxations and segmental motions of the polymer blend. As the amorphous region progressively increases (region-II), however, the polymer chain acquires faster internal modes in which bond rotations produce segmental motion. This, in turn, favors the hopping inter-chain and intra-chain ion movements and the conductivity of the polymer blend electrolyte thus become high. Similar behavior has been reported on poly(vinyl alcohol) based electrolyte films [31,32] and PEO based polymer electrolyte films [33–37]. The variation of electrical conductivity (σ) as a function of temperature (T) in the entire temperature range can be fitted to the relation [38]:

$$\sigma = \sigma_o \exp(-E_a/kT) \qquad (2)$$

where σ_o is a constant, k, the Boltzmann constant and E_a, the activation energy. The calculated activation energies (E_a) in the two regions for (PVC + PEO + KBr) complexes are summarized in Table 2.

The activation energy values of different polymer blend electrolytes were calculated from the slopes of linear fit of Arrhenius plots of different polymer blend electrolytes. The activation energy is a combination of energy of charge carrier creation (defect formation) and the energy of ion migration that can be evaluated by linear fitting to the log(σ) vs. 1000/T plots [39,40]. Therefore, it can be suggested that the value of E_a is due to the energy that is required to provide a conductive condition for the migration of ions. The activation energy is found to decrease gradually with increasing KBr salt concentration.

3.4. Optical analysis

Measurement of the absorption spectrum is the most direct and simplest method for investigating the band structure of materials. In the absorption process an electron is excited from a lower to higher energy state by absorbing a photon of known energy in the transmitting radiation. The changes in the transmitted radiation can decide the types of possible electron transitions. Fundamental absorption refers to band-to-band or exciting transition.
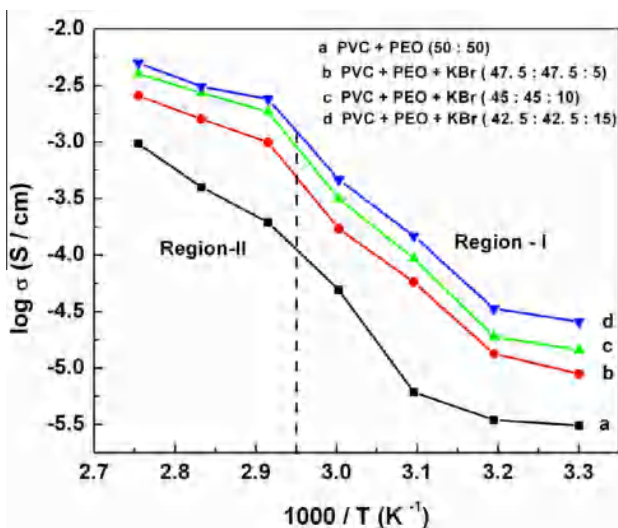
Table 1
Conductivity at different temperatures of (PVC + PEO + KBr) solid polymer blend electrolyte system.

Polymer blend electrolyte system (wt%)	Conductivity (σ), S cm^{-1}			
	303 K	323 K	343 K	363 K
PVC + PEO (50:50)	3.09×10^{-6}	4.84×10^{-6}	1.94×10^{-4}	8.23×10^{-4}
PVC + PEO + KBr (47.5:47.5:5)	8.88×10^{-6}	5.77×10^{-5}	9.94×10^{-4}	2.57×10^{-3}
PVC + PEO + KBr (45:45:10)	1.44×10^{-5}	9.29×10^{-5}	1.85×10^{-3}	4.01×10^{-3}
PVC + PEO + KBr (42.5:42.5:15)	2.56×10^{-5}	1.46×10^{-4}	2.41×10^{-3}	5.01×10^{-3}

Table 2
Absorption edge, optical band gap (both direct and indirect) and activation energy values of undoped and KBr doped (PVC + PEO) polymer blend films.

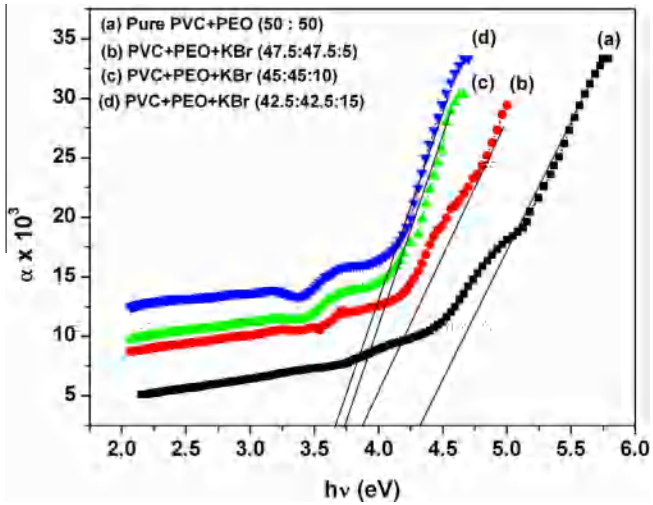| Polyblend electrolyte system (wt%)	Absorption edge (eV)	Optical band gap (eV)		Activation energy (eV)	
		Direct	Indirect	Region-I	Region-II
PVC + PEO (50:50)	4.30	4.10	4.15	0.66	0.79
PVC + PEO + KBr (47.5:47.5:5)	3.89	3.62	3.83	0.33	0.53
PVC + PEO + KBr (45:45:10)	3.75	3.52	3.76	0.25	0.49
PVC + PEO + KBr (42.5:42.5:15)	3.66	3.45	3.63	0.20	0.30

Fig. 6. α vs. $h\upsilon$ (photon energy) plots of (a) pure PVC + PEO (50:50); (b) PVC + PEO + KBr (47.5:47.5:5); (c) PVC + PEO + KBr (45:45:10); (d) PVC + PEO + KBr (42.5:42.5:15) films.

Furthermore the fundamental absorption manifests itself by a rapid rise in absorption, known as absorption edge, which can be used to determine the optical band gap. Insulators/semiconductors are generally classified into two types: (a) direct band gap and (b) indirect band gap. In direct band gap semiconductors, the top of the valance band and the bottom of the conduction band both lie at same zero crystal momentum (wave vector). If the bottom of the conduction band does not correspond to zero crystal momentum, then it is called indirect band gap semiconductor. In indirect band gap materials transition from valence to conduction band should always be associated with a phonon of the right magnitude of crystal momentum. Davis and Shalliday [41] reported that near the fundamental band edge, both direct and indirect transitions occur and can be observed by plotting $\alpha^{1/2}$ and α^2 as a function of energy ($h\upsilon$). The analysis of Thutpalli and Tomlin [42] is based on Eqs. (3) and (4):

$$(h\upsilon n\alpha)^2 = C_1(h\upsilon - E_{gd}) \tag{3}$$

$$(h\upsilon n\alpha)^{1/2} = C_2(h\upsilon - E_{gi}) \tag{4}$$

where $h\upsilon$ is the photon energy, E_{gd}, the direct band gap, E_{gi}, the indirect band gap, n, the refractive index, α, the absorption coefficient and C_1, C_2 are constants. These expressions can be applied to both direct and indirect transitions and are helpful in the determination of the band structure of materials. When a direct band gap exists, the absorption coefficient has the subsequent dependence on the energy of the incident photon [38,43],

$$(\alpha h\upsilon) = C(h\upsilon - E_g)^{1/2} \tag{5}$$

where E_g is the band gap, C, is a constant dependent on the specimen structure, α is the absorption coefficient, υ is the frequency of the incident light, and h, the Planck's constant. To determine the nature and width of the band gap, α, was plotted as a function of photon energy ($h\upsilon$) (Fig. 6) and the absorption edge values were obtained by extrapolating the linear portions of the curves to zero absorption value. It was observed that the absorption edge for pure (PVC + PEO) polyblend film lies at 4.30 eV whereas for 5, 10 and 15 wt% KBr doped (PVC + PEO) polyblend films the absorption edge lies at 3.89, 3.75 and 3.66 eV, respectively (Fig. 6).

The optical band gaps were evaluated from $(\alpha h\upsilon)^2$ and $(\alpha h\upsilon)^{1/2}$ vs. $h\upsilon$ (photon energy) plots and the allowed direct transition energies were determined by extrapolating the linear portion of the curves to zero absorption. For pure (PVC + PEO) polyblend electrolyte the direct and indirect band gap values are similar to as α vs. $h\upsilon$ (photon energy) while for 5, 10 and 15 wt% KBr doped (PVC + PEO) electrolyte, the similar optical band gap values as α vs. $h\upsilon$ (photon energy). For indirect transitions, which require photon assistance, the absorption coefficient has the subsequent dependence on the photon energy:

$$\alpha h\upsilon = A(h\upsilon - E_g + E_p)^2 + B(h\upsilon - E_g - E_p)^2 \tag{6}$$

where E_p is the energy of the photon associated with the transition and A and B are constants depending on the band structure.
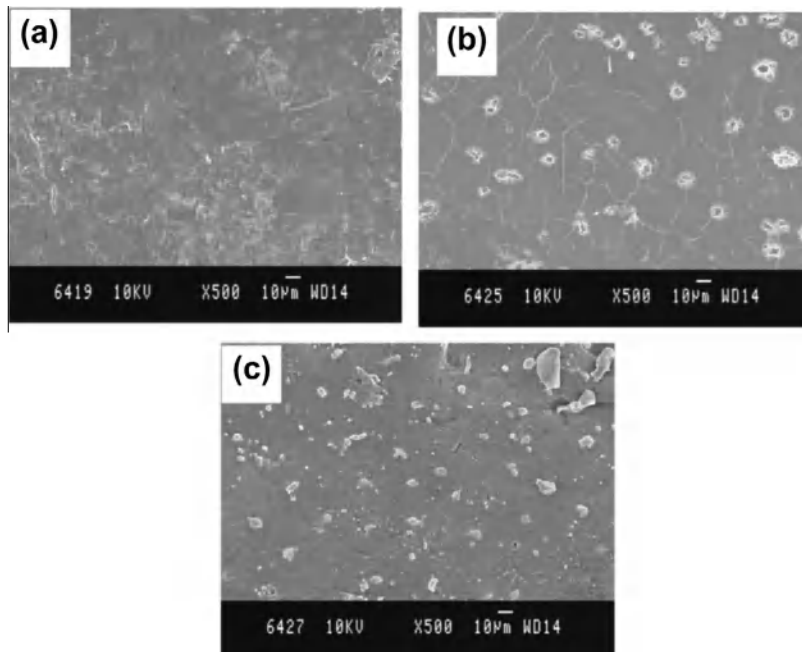

Fig. 7. SEM photographs of (a) pure PVC + PEO (50:50); (b) PVC + PEO + KBr (47.5:47.5:5); (c) PVC + PEO + KBr (42.5:42.5:15).

These values are tabulated in Table 2 together with the absorption edge values, the direct band gap energies and the activation energies obtained from conductivity measurements.

The decrease in optical band gap/activation energy on doping may be explained on the basis of the fact that the incorporation of small amounts of dopant forms charge transfer complexes (CTCs) in the host lattice. These CTCs increase the electrical conductivity by providing additional charges in the lattice [44]. This results in a decrease of activation energy. The conductivity data showed a small comparison with optical band gap energies. The band edge, direct band gap and indirect band gap values shifted to lower energies on doping with KBr. The wide variation in the magnitudes of the optical band gap vis-a-vis the activation energies may be attributed to the fact that their nature is different. While the activation energy corresponds to the energy required for conduction from one site to another, the optical band gap corresponds to inter band transition [43].

The morphology of the pure (PVC + PEO) and (PVC + PEO + KBr) (47.5:47.5:5), (42.5:42.5:15) polymer blend electrolytes, studied by the SEM technique, is of a uniform type, but with different degrees of roughness (Fig. 7(a)–(c)). This suggests that the PVC and PEO molecules may disperse in the soft-segment phase with little influence on the microphase separation and mixing of the hard and soft segments. The increase of the degree of roughness with increased KBr concentration indicates segregation of the dopant in the host matrix.

4. Conclusions

The increase in conductivity with increasing concentration of KBr is attributed to the decrease in the degree of crystallinity and increase in the degree of amorphosity. The calculated activation energies in both regions show a decrease in their value with increasing dopant concentration of KBr. Optical absorption edge and optical energy gap (both direct and indirect) showed decreasing trend with increased concentration. Thermal characteristics of pure (PVC + PEO) and for different compositions of (PVC + PEO + KBr) polyblend electrolyte have been assessed by thermal analysis method. An increasing dopant concentration decreases the melting temperature due to reduced dipole interactions in its homopolymers. This data revealed that the present electrolyte system is a viable candidate for electrochemical device applications such as high-performance solid-state batteries, smart windows, chemical sensors, microelectronic, electrochromic devices and variable reflectance mirrors.

Acknowledgements

References

[1] A. Manuel Stephan, R. Thirunakaran, N.G. Renganathan, V. Sundram, S. Pitchumani, N. Muniyandi, J. Power Sources 82 (1999) 752–758.
[2] S. Ramesh, A.K. Arof, Solid State Ionics 136–137 (2000) 1197–1200.
[3] A. Manuel Stephan, T. Prem Kumar, N.G. Renganathan, S. Pitchumani, R. Thirunakaran, N. Muniyandi, J. Power Sources 89 (2000) 80–87.
[4] S. Ramesh, A.H. Yahaya, A.K. Arof, Solid State Ionics 152–153 (2002) 291–294.
[5] J.R. Mac Callum, C.A. Vincent (Eds.), Polymer Electrolyte Reviews, Elsevier, Amsterdam, 1987.
[6] K. Murata, Electrochim. Acta 40 (1995) 2177.
[7] M.B. Armand, in: J.R. Mac Callum, C.A. Vincent (Eds.), Polymer Electrolyte Reviews, Elsevier, Amsterdam, London, 1987, p. 1.
[8] M. Jaipal Reddy, Peter P. Chu, Electrochim. Acta 47 (2002) 1189–1196.
[9] J. Siva Kumar, A.R. Subramanyan, M. Jaipal Reddy, U.V. Subba Rao, Mater. Lett. 60 (2006) 3346–3349.
[10] A.L. Oleksiak, H.D. Inerowicz, J. Power Sources 813 (1999) 81–82.
[11] S.A. Hashmi, A. Chandra, S. Chandra, in: B.V.R. Chowdari et al. (Eds.), Solid State Ionics, Materials and Applications, World Scientific, Singapore, 1992, p. 567.
[12] T. Sreekanth, M. Jaipal Reddy, S. Subramanyam, U.V. Subba Rao, Mater. Sci. Eng. B 64 (1999) 107.
[13] T. Sreekanth, M. Jaipal Reddy, S. Ramalingaiah, U.V. Subba Rao, J. Power Sources 79 (1999) 105.
[14] P.S. Anantha, K. Hariharan, Solid State Ionics 176 (2005) 155.
[15] P.A.R.D. Jayathilaka, M.A.K.L. Dissanayake, I. Albinsson, B.E. Mellander, Electrochim. Acta 47 (2002) 3257.
[16] X.Q. Yang, H.S. Lee, L. Hanson, J. McBreen, Y. Okamoto, J. Power Sources 54 (1995) 198.
[17] A.L. Gopalan, P. Santhosh, K.M. Manesh, J.H. Nho, S. Chul-Gyun Hwang, K.P. Lee, J. Membr. Sci. 325 (2008) 683.
[18] B.P. Tripathi, V.K. Shahi, Polym. Sci. 36 (2011) 945.
[19] A. Bhide, K. Hariharan, Eur. Polym. J. 43 (2007) 4253.
[20] N. Manuel Stephan, Yuria Saito, N. Muniyandi, N.G. Renganathan, S. Kalyanasundarm, R. Nimma Elizabeth, Solid State Ionics 148 (2002) 467.
[21] T. Uma, U. Mahalingam, Stimmeng, J. Mater. Sci. 39 (2004) 2897.
[22] S. Ahmad, H.B. Bohidar, S. Ahmad, S.A. Agnihotry, Polymer 47 (2006) 3583–3590.
[23] W. Qiu, X. Ma, Q. Yang, Y. Fu, X. Zong, J. Power Sources 138 (2004) 245–252.
[24] S. Ramesh, Tan Winie, A.K. Arof, Eur. Polym. J. 43 (2007) 1963–1968.
[25] R.M. Hodge, G.H. Edward, G.P. Simon, Polymer 37 (1996) 1371.
[26] V. Madhu Mohan, V. Raja, A.K. Sharma, V.V.R. Narasimha Rao, Mater. Chem. Phys. 94 (2004) 177.
[27] A.A. Mohamad, N.S. Mohamad, M.Z.A. Yahya, R. Othman, S. Ramesh, Y. Alias, A.K. Aroof, Solid State Ionics 156 (2003) 171.
[28] S.A. Hashmi, A. Kummar, K.K. Maurya, S. Chandra, J. Phys. D: Appl. Phys. 23 (1990) 1307.
[29] F. Croce, S. Sacchetti, B. Scrosati, Power Sources 161 (2006) 560.
[30] P.K.C. Pillai, P. Khurana, A. Trilateral, Mater. Sci. Lett. 5 (1986) 629.
[31] S.L. Agrawal, P.K. Shukla, Ind. J. Pure Appl. Phys. 38 (2000) 53.
[32] R. Chandrasekaran, I.R. Mangani, R. Vasanthi, S. Selladurai, Bull. Electrochem. 17 (2001) 249.
[33] M. Armand, J.M. Chabagno, M. Duclot, in: P. Vashista, J.N. Mudy, G. Shenoy (Eds.), Fast Ion Transport in Solids, North Holland, New York, 1979, p. 131.
[34] F. Bonino, B. Scrosati, in: B.V.R. Chowdari, S. Radhakrishna (Eds.), Polymeric Electrolytes in Materials for Solid State Batteries, World Scientific, Singapore, 1986, p. 42.
[35] S. Sreepathi Rao, M. Jaipal Reddy, E. Laxminarasaiah, U.V. Subba Rao, Mater. Sci. Eng. B 33 (1995) 173.
[36] K.K. Maurya, N. Srivastava, S.A. Hashmi, S. Chandra, J. Mater. Sci. 27 (1992) 6357.
[37] T. Sreekanth, M. Jaipal Reddy, S. Ramalingaiah, U.V. Subba Rao, J. Power Sources 79 (1999) 105.
[38] J.G. Simmons, in: L.I. Maissel, R. Glang (Eds.), Hand Book of Thin Film Technology, McGraw-Hill, New York, 1970.
[39] L. Famiza, A. Madzlan, K. Nasir, A.M.M. Ali, Z.Y. Muhd, J. Power Sources 159 (2006) 1401.
[40] M.J. Reddy, T. Sreekanth, U.V.S. Rao, Solid State Ionics 126 (1999) 55.
[41] D.S. Davis, J.S. Shalliday, Phys. Rev. 118 (1960) 1020.
[42] G.M. Thutulpalli, S.G. Tomlin, J. Phys. D: Appl. Phys. 9 (1976) 1639.
[43] C. Uma Devi, A.K. Sharma, V.V.R.N. Rao, Mater. Lett. 56 (2002) 167.
[44] V. Raja, A.K. Sharma, V.V.R. Narasimha Rao, Mater. Lett. 57 (2003) 4678.